Hindawi
International Journal of Aerospace Engineering
Volume 2020, Article ID 8846177, 15 pages
https://doi.org/10.1155/2020/8846177

Research Article

A Study on Dynamic Characteristics of Satellite Antenna System considering 3D Revolute Clearance Joint

Zhengfeng Bai and Jijun Zhao

Department of Mechanical Engineering, Harbin Institute of Technology, Weihai 264209, China

Correspondence should be addressed to Zhengfeng Bai; baizhengfeng@126.com

Received 10 June 2020; Revised 3 August 2020; Accepted 7 August 2020; Published 28 August 2020

Academic Editor: Angelo Cervone

Clearances in the joints of real mechanisms are unavoidable due to assemblage, manufacturing errors, and wear. The dual-axis driving and positioning mechanism is one kind of space actuating mechanism for satellite antenna to implement precise guidance and positioning. However, in dynamics analysis and control of the satellite antenna system, it is usually assumed that the revolute joint in the satellite antenna system is perfect without clearances or imperfect with planar radial clearance. However, the axial clearance in an imperfect revolute joint is always ignored. In this work, the revolute joint is considered as a 3D spatial clearance joint with both the radial and axial clearances. A methodology for modeling the 3D revolute joint with clearances and its application in satellite antenna system is presented. The dynamics modeling and analysis of the satellite antenna system are investigated considering the 3D revolute clearance joint. Firstly, the mathematical model of the 3D revolute clearance joint is established, and the definitions of the radial and axial clearance are presented. Then, the potential contact modes, contact conditions, and contact detection of the 3D revolute clearance joint are analyzed. Further, the normal and tangential contact force models are established to describe the contact phenomenon and determine the contact forces in the 3D revolute clearance joint. Finally, a satellite antenna system considering the 3D revolute clearance joint with spatial motion is presented as the application example. Different case studies are presented to discuss the effects of the 3D revolute clearance joint. The results indicate that the 3D revolute clearance joint will lead to more severe effects on the dynamic characteristics of the satellite antenna system. Therefore, the effects of axial clearance on the satellite antenna system cannot be ignored in dynamics analysis and design of the satellite antenna system.

1. Introduction

The dual-axis driving and positioning mechanism is one kind of actuating mechanism for a satellite antenna to meet precise pointing requirements. Generally, in dynamics analysis and control of the satellite antenna system, it is usually assumed that the revolute joint in the satellite antenna system is perfect without clearances or imperfect with planar radial clearances. The axial clearance in the revolute joint is always ignored [1–5]. However, clearances always exist in a real joint due to due to assemblage, manufacturing errors, and wear. Clearances will induce contact and impact in joints, which cause vibration and affect the dynamic performances of the real mechanical systems [6–13]. The effects of clearances on dynamic responses of mechanisms have been studied by many researchers [14–22].

Flores [23] presented a dynamics analysis of a planar linkage mechanism with clearances considering different parameters, such as clearance size and driving speed. Zhao and Bai [24] studied the dynamic characteristics of a space robot manipulator with one planar revolute clearance joint. The nonlinear equivalent spring-damper model is established for the normal contact model in joint clearance. The friction effect is considered using the Coulomb friction model. Erkaya and Uzmay [25, 26] presented a study on decreasing the deviations arising from a clearance joint in planar linkage mechanisms by a neural network-genetic algorithm procedure. Muvengei et al. [27] investigated the

dynamics and motion modes of a slider-crank mechanism with two planar revolute clearance joints. Bai and Sun [28] studied the dynamic responses of a planar mechanism system including three planar revolute clearance joints. Different contact modes caused by the multiclearance joints were investigated. Wang et al. [29] presented a nonpenetration approach of frictional contact analysis for modeling revolute clearance joints of planar rigid multibody systems. Zhang and Zhang [30] proposed a method to minimize the influence of revolute joint clearance of a redundantly actuated mechanism. A planar 3 DOF redundantly actuated 4RRR mechanism with 8 clearance joints was applied as an illustration. Salahshoor et al. [31] studied the effect of joint stiffness on the vibration behavior of a typical slider-crank mechanism with a flexible component and joint clearances. Wang et al. [32] studied the dynamic responses of planar multibody systems with dry revolute clearance joint considering the radial clearance via numerical and experimental approaches. Tan et al. [33] investigated the effects of friction on the dynamic behavior of a planar crank-slider mechanism considering a revolute joint with radial clearance using the LuGre friction model. Chen et al. [34] analyzed the effect of multiple clearances and different friction models on the dynamic behavior of a planar multi-DOF mechanism. The 2 DOF nine-bar planar mechanism was used as the application example. Li et al. [35] investigated the dynamic behavior of a planar rigid-flexible coupling solar array system considering joint clearance numerically. A typical solar array model was used as the application example. Wang and Wang [36] studied the dynamics model of a 4-SPS/PS parallel mechanism with a flexible actuated rod and clearance spherical joint. Pi and Zhang [37] presented a study of dynamics analysis of the classical planar slider-crank mechanism with multiple revolute clearance joints. A general multiple patch-based revolute clearance joint model was proposed. Amiri et al. [38] proposed a control scheme to restrain the clearance and maintain a more stable behavior of planar mechanisms. The approach was based on using a tuned mass damper to reduce the effects of clearances in mechanisms for the passive control purpose. Zhan et al. [39] presented a unified motion reliability analysis method for general planar parallel manipulators with interval clearance variables of revolute and prismatic joints. Two typical types of PPMs, the 3RRR PPM and 3PRR PPM, were analyzed as examples. Guo et al. [40] presented a dynamics model to investigate the position secondary motion considering all associated joint clearances. Chen et al. [41] proposed a general methodology for modeling and evaluating the dynamic characteristics of planar multibody systems considering the revolute clearance joints and performed the relevant experimental verification. Erkaya [42] studied the effects of planar clearance on motion accuracy of a six DOF robot system. Different scenarios for clearance values and working periods were performed to fulfil the required motion task of the robot.

Besides, many studies also have been focused on the topics of mechanism with clearance joints considering parameter uncertainty [43–47], joint wear [48, 49], design optimization [50], joint lubrication [51, 52], flexible body [53, 54], nonlinear analysis [55], joint friction [56, 57], and other topics [58–60]. All the researches indicated that clearance leads to significant effects on dynamic response of mechanism systems. Further, based on the studies of mechanisms with a planar revolute clearance joint, recently, researchers are focused on 3D revolute clearance joints [61–65]. Flores et al. [61] presented a technique for assessing the influences of radial clearance of spatial revolute joints on the kinematics and dynamics of multibody systems. Four different possible motion scenarios of the journal relative to the bearing were considered. However, the axial clearance was not considered in the revolute joint. Brutti et al. [62] presented a study of the mechanism with one 3D revolute joint considering 4 contact configurations. More recently, Yan et al. [63], Marques et al. [64], and Isaac et al. [65] also presented studies of mechanisms with a 3D revolute clearance joint. These researches indicated that there will be more contact modes in a 3D revolute clearance joint.

In fact, due to the manufacturing and assembling errors, axial clearances always exist in revolute joints, which have been less considered. Most of the previous studies focused on the dynamic responses of mechanisms with planar radial clearances, while axial clearances will result in relative motion along the axial direction between the journal and the bearing of a 3D revolute clearance joint. Correspondingly, it will lead to a more complex contact phenomenon when both the radial and axial clearances are considered. Also, for a highly precise space mechanism with spatial motion, the effects of axial clearance in a revolute joint cannot be ignored.

The dynamics model and simulation of mechanisms considering only radial clearance were widely presented in the literature. Thus, the objective of this work is to study the dynamic characteristics of the space mechanism system considering both the radial and axial clearances in a 3D revolute clearance joint. A methodology for modeling the 3D revolute joint with clearances and its application in satellite antenna system is presented. The contribution of this paper can be summarized as follows: (1) The revolute joint considered in this paper is a spatial joint with both the radial and axial clearances. The mathematic model of the 3D revolute clearance joint is established, and different contact scenarios are presented and discussed. (2) The 3D revolute clearance joint model presented in this work is applied to a high-precision mechanism with spatial motion on spacecraft. The effect of the 3D clearance joint on dynamic performances of a satellite antenna is investigated. Different case studies are presented to discuss the effects of axial clearance. (3) This work develops the model of the revolute clearance joint, and the 3D revolute clearance is more in line with the actual situation of the real revolute joint. Therefore, the three-dimensional methodology of the clearance revolute joint proposed in this paper improves the model of the revolute clearance joint and leads to a more accurate result.

To this end, different case studies are presented to discuss the effects of the 3D revolute clearance joint. Firstly, the mathematic model of the 3D revolute clearance joint is established considering the radial and axial clearances. The definitions of the radial and axial clearances are presented. Then, the potential contact scenarios, contact conditions,

and contact detection of the 3D revolute clearance joint are analyzed. The potential contact scenarios can reveal the different contact phenomena in the 3D revolute clearance joint. The minimum distances between the journal and the bearing in both the axial and radial directions are obtained to determine the contact conditions and detections. Further, the normal and tangential contact force models are established to describe the contact phenomenon and determine the contact forces in the revolute clearance joint. Finally, a satellite antenna system with spatial motion is presented as the demonstrative application example. The dynamic characteristics of the satellite antenna system are investigated considering both the radial and axial clearances in a 3D revolute clearance joint.

2. Model of Revolute Joint with Radial and Axial Clearances

2.1. Definition of Ideal 3D Revolute Joint without Clearances. The 3D revolute joint without clearance between bodies i and j is shown in Figure 1. Any point on the axis of the revolute joint has constant coordinates in both local coordinate systems. P_0 is an arbitrary point on the joint axis. Two other points, P_i on body i and P_j on body j, are also chosen as arbitrary points on the joint axis. It is clear that vectors $\mathbf{s}_i$ and $\mathbf{s}_j$ must remain parallel. Therefore, there are five constraint equations for a 3D revolute joint without clearance:

$$\begin{aligned} &\mathbf{r}_i + \mathbf{A}_i\mathbf{s}_i^P - \mathbf{r}_j - \mathbf{A}_j\mathbf{s}_j^P = 0, \\ &\mathbf{s}_i \times \mathbf{s}_j = \tilde{\mathbf{s}}_i\mathbf{s}_j = 0, \end{aligned} \tag{1}$$

where $\mathbf{A}_i$ and $\mathbf{A}_j$ are the transformation matrices that define the orientation of bodies i and j, respectively. $\tilde{\mathbf{s}}_i$ is the skew-symmetric matrix associated with the vector $\mathbf{s}_i$.

Thus, the revolute joint without clearances is described by a set of holonomic algebraic constraints. There is only one relative degree of freedom (DOF) between two bodies connected by a 3D ideal revolute joint without clearance.

2.2. Definition of 3D Revolute Joint with Clearances. Figure 2 shows the configuration of a 3D revolute joint with both the radial and axial clearances. Comparing with the ideal 3D revolute joint without clearances, although a revolute joint with clearances does not restrict any degrees of freedom, it limits the journal to move within the bearing. When both the radial and axial clearances are presented in a 3D revolute joint, the dynamics of the clearance joint are controlled by contact forces applied on the journal and bearing. Therefore, in this work, the mechanical bodies connected by the 3D revolute clearance joint are modelled as contact rigid bodies. And consequently, contact-impact forces control the dynamics of the clearance joint. Therefore, the constraints of the revolute clearance joint are modelled as contact force constraints.

The components of the 3D revolute clearance joint are idealized as two cylinders, where the journal is considered as a cylinder with an end flange. According to the geometric description, as shown in Figure 1(a), the axial clearance C_a

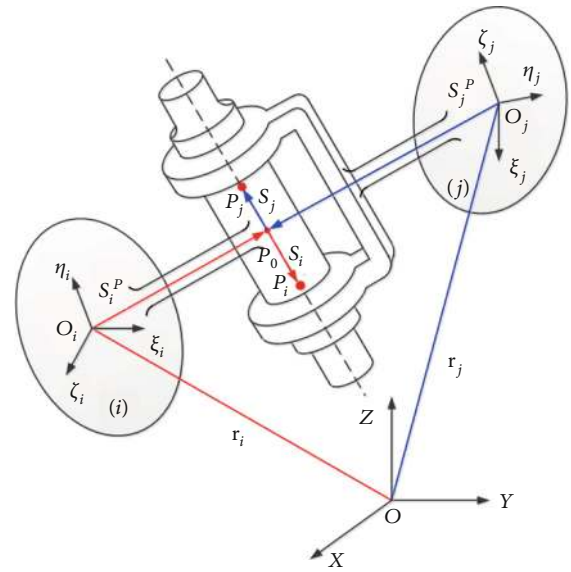

Figure 1: 3D revolute joint connecting bodies i and j.

and the radial clearance C_r between the journal and the bearing are defined as follows:

$$\begin{aligned} C_a &= \frac{L_j - L_i}{2}, \\ C_r &= R_i - R_j, \end{aligned} \tag{2}$$

where L_j and R_j are the length and the radius of the journal, respectively. L_i and R_i are the length and the radius of the bearing, respectively.

In Figure 2(b), two local coordinate systems O_j-$x_jy_jz_j$ and O_i-$x_iy_iz_i$ are attached to the journal and bearing, respectively. Axis z_j and axis z_i are along to the central axes of the journal and bearing, respectively. O_j is the geometric center of the journal, and O_i is the center of the end face circle of the bearing. Additionally, a global coordinate system O-XYZ is fixed to the ground. Initially, the three coordinate systems keep the same orientation. Therefore, the relative motion between the journal and the bearing is equivalent to the relative motion between the two local coordinate systems O_j-$x_jy_jz_j$ and O_i-$x_iy_iz_i$, which are fixed to the journal and bearing, respectively.

2.3. Contact Scenarios in 3D Revolute Clearance Joint. Considering that both the axial and radial clearances exist in such a 3D revolute joint, the contacts of the journal and bearing in the axial and radial directions are independent. Therefore, it may contact in the axial direction, radial direction, or both directions. In terms merely of the radial clearance condition, four potential contact scenarios in the radial direction can be recognized, that is, no contact, one-point contact, two-point contact, and line contact. Similarly, when considering the axial clearance separately, there are also four potential contact scenarios in the axial direction, that is, no contact, one-point contact, two-point contact, and surface contact.

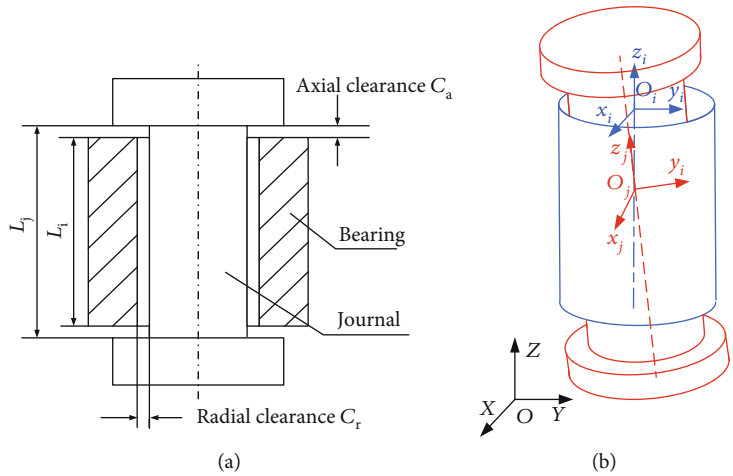

FIGURE 2: Configuration of 3D revolute joint with radial and axial clearances ((a) configuration of the revolute joint with clearances; (b) the geometric description for the 3D revolute joint).

Furthermore, 13 potential contact scenarios, as shown in Figure 3, can be found when both the axial and radial clearances are considered in a 3D revolute clearance joint. It should be noted that the joint's behavior is the function of these 13 scenarios which depends on joint geometry and the dynamics configuration of the system. Thus, some of these potential cases can be eliminated and not further happen.

2.4. Contact Conditions. The potential contact points on the journal and bearing are shown in Figures 4 and 5, which are simplified to calculate the minimum radial and axial distances, respectively [63].

From Figure 4, it can be observed that the potential contact points in the radial direction must be on the two circles of the bearing end face. The centers of the end faces of the journal are point M and point N, respectively. The centers of the end faces of the bearing are point O_i and point O_i', respectively. The vector $\mathbf{d}_2^{j'}$ with orientation from O_j to O_i connects the origins of the local coordinate systems O_j-$x_jy_jz_j$ and O_i-$x_iy_iz_i$. $\mathbf{d}_2^j$ denotes the projection of $\boldsymbol{d}_2^{j'}$ on the cross section of the journal. The coordinates of points O_i, O_i', O_j, M, and N at the global coordinate systems at time t are defined as $O_i(t) = (x_i, y_i, z_i)^T$, $O_i'(t) = (x_i', y_i', z_i')^T$, $O_j(t) = (x_j, y_j, z_j)^T$, $M(t) = (x_M, y_M, z_M)^T$, and $N(t) = (x_N, y_N, z_N)^T$. Further, through the center of the section O_t, a vector $\mathbf{d}_1^j$ perpendicular to the vector $\mathbf{d}_2^j$ is made. Then, the tangent plane τ_1 of the journal flank is acquired, which is parallel to the vector $\mathbf{d}_1^j$. The tangent plane τ_1, journal flank, and cross section intersect at one point, and the intersection point is defined as point P. The tangent plane τ_2 of the end face circle of the bearing is parallel to the vector $\mathbf{d}_1^j$ and the tangent point is defined as Q. Therefore, the tangent plane τ_1 is parallel to the tangent plane τ_2. Further, it can be found that point Q is the potential contact point. Obviously, the radial minimum distance between the journal and the bearing at the left side equals the distance between the planes τ_1 and τ_2 [63, 66].

Therefore, the calculation of the minimum distance in the radial direction can be expressed as follows:

$$\delta_r = R_i \cdot \cos\theta - R_j - \left|\mathbf{d}_2^j\right|, \tag{3}$$

where δ_r represents the minimum distance between the journal and bearing in the radial direction. θ is the angle between lines O_iQ and O_iP, as shown in Figure 4.

$$\begin{aligned} \mathbf{d}_2^j &= O_i - O_t, \\ \mathbf{d}_2^{j'} &= O_i - O_j, \\ \mathbf{d}_2^{j''} &= O_t - O_j, \\ \left|\mathbf{d}_2^j\right| &= \sqrt{\left(\mathbf{d}_2^j\right)^T \mathbf{d}_2^j}. \end{aligned} \tag{4}$$

In particular, in the case where the axes of the journal and the bearing are parallel to each other, the angle θ becomes zero. Then, (3) can be expressed as

$$\delta_r = R_i - R_j - \left|\mathbf{d}_2^j\right|. \tag{5}$$

Further, the contact condition of the journal and bearing in the radial direction can be expressed as

$$\begin{cases} \delta_r > 0, & \text{free motion in radial direction,} \\ \delta_r \le 0, & \text{contact and impact in radial direction.} \end{cases} \tag{6}$$

Similarly, the potential contact point on the journal and bearing along the axial direction is depicted in Figure 5, which is employed to calculate the minimum axial distance between the journal and bearing. It can be seen that axial contact occurs between the end flange of the journal and the end face of the bearing. It should be noted that the wall thickness of the actual bearing should be taken into account.

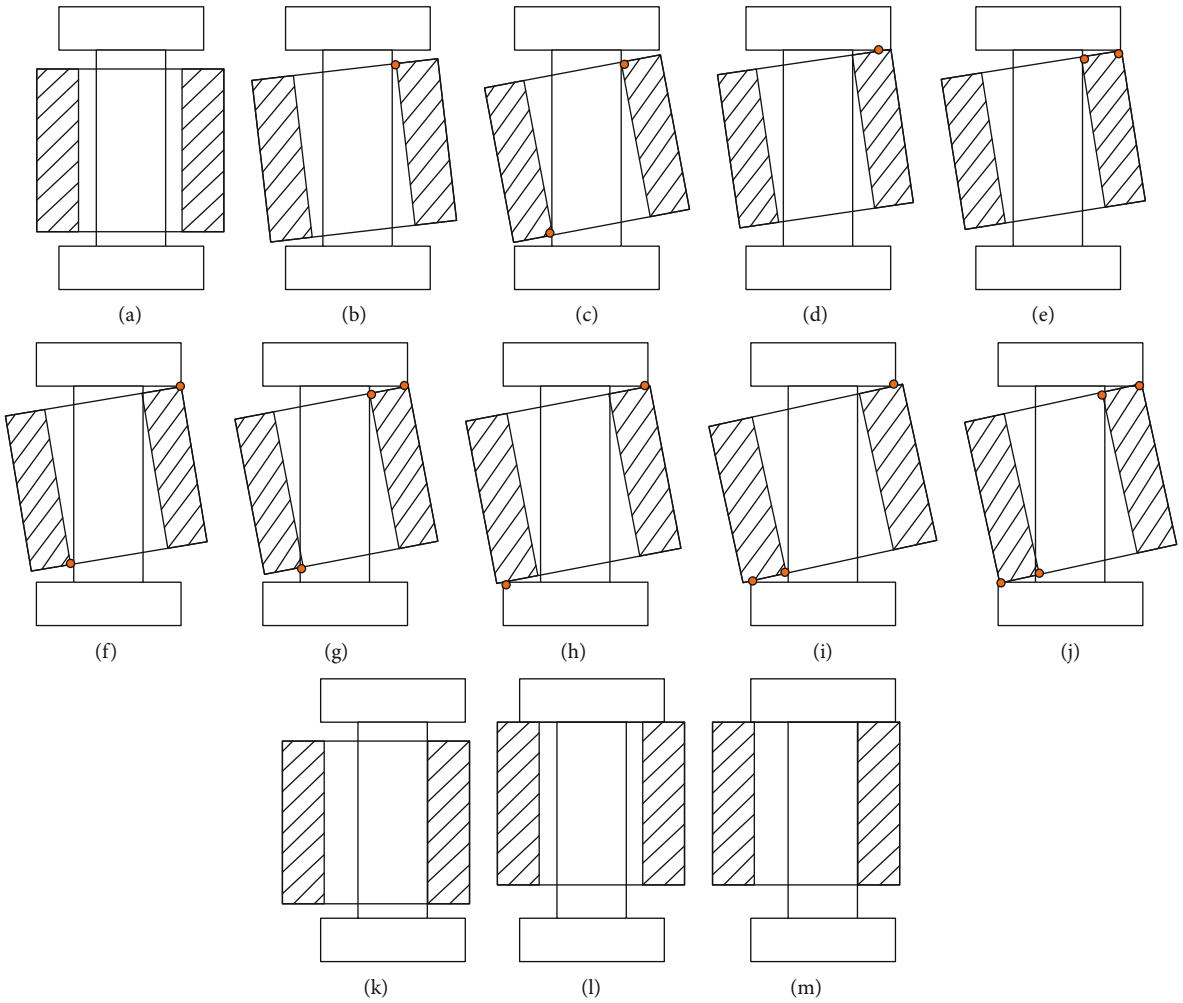

Figure 3: Contact scenarios of revolute joint with 3D clearances.

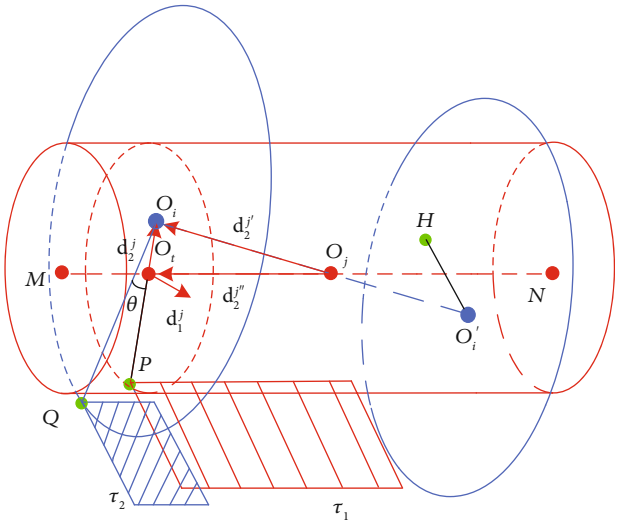

Figure 4: Mathematical model of radial distance of revolute joint with 3D clearance.

In order to calculate the minimum radial distance, plane τ_2 is tangent to the left end face circle of the outer surface of the bearing at point Q', which is the potential contact point for calculating the minimum axial distance. Further, it can be found that the distance between the point Q' and the end flange is the minimum distance along the axial direction, which can be expressed as [63]

$$\delta_a = \frac{L_j}{2} - a - b = \frac{L_j}{2} - \left|\mathbf{d}_2^{j''}\right| - R_{io} \cdot \sin\theta, \tag{7}$$

where δ_a represents the minimum distance between the journal and bearing in the axial direction. a is the norm of vector $\mathbf{d}_2^{j''}$. b is the projection of R_{io} on the journal axis, as shown in Figure 5.

Therefore, the contact condition in the axial direction can be expressed as

$$\begin{cases} \delta_a > 0, & \text{free motion in axial direction,} \\ \delta_a \le 0, & \text{contact and impact in axial direction.} \end{cases} \tag{8}$$

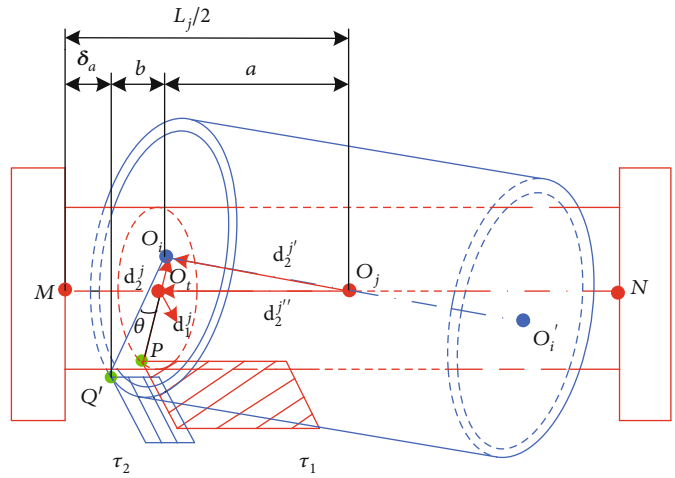

Figure 5: Mathematical model of axial distance of revolute joint with 3D clearance.

2.5. Contact Detection. Contact detection is one of the most important aspects in contact analysis. Since the contact-impact phenomena in the radial and axial directions are independent in the 3D revolute clearance joint, a separate condition is employed to deal with the contact detection in each direction. Based on the minimum radial and axial distances, the contact detection between the journal and bearing can be judged according to the positive and negative values of the distances. Theoretically, the radial or axial distance is equal to zero at the switching instantaneous moment, but it cannot be accurately found in the numerical simulation. Therefore, in numerical simulation, the sign of the minimum distance could reveal the change of contact status. When the minimum distance changes sign from time t to $t + \Delta t$, contact must occur and the contact can be detected by

$$\delta_a(t) \cdot \delta_a(t + \Delta t) \le 0, \tag{9}$$

$$\delta_r(t) \cdot \delta_r(t + \Delta t) \le 0. \tag{10}$$

When at least one of the equations is satisfied, contact will occur during t to $t + \Delta t$. It should be noted that the contact could occur in the radial and axial directions simultaneously.

Therefore, contact is detected when at least one of Equations (9) and (10) is verified. An alternative way to determine the presence of contact for multiple time-step size integrators is using the characteristics of the integration algorithm selected. The step size is proposed to reach smaller values to keep the integration tolerance error. Thus, the impact velocity and the direction of the contact can be predicted in the overall system motion.

3. Contact Force Models

Usually, there will always be contact/impact in a real joint with clearances in mechanisms, which includes normal contact forces and tangential friction forces simultaneously. Tian et al. [67] presented a comprehensive survey of dynamics of multibody mechanical systems with clearance or imperfect joints, in which the contact force model used for modeling the clearance joint is discussed. Therefore, to evaluate the contact forces efficiently between the bearing and the journal for a revolute joint with clearance, special attention must be given to the numerical description of the contact force model [68–73]. There have been several normal contact force models used to determine the contact forces in a clearance joint.

In this work, the Lankarani and Nikravesh [72] contact force model is used to describe the normal contact of clearance joint, and it is expressed as

$$F_n = K\delta^n \left[1 + \frac{3\left(1 - c_e^2\right)\dot{\delta}}{4\dot{\delta}^{(-)}}\right], \tag{11}$$

where δ is the deformation, $\dot{\delta}$ is the relative deformation velocity, c_e is the coefficient of restitution, and $\dot{\delta}^{(-)}$ is the initial normal relative velocity of the impact point. K is the contact stiffness coefficient and it is obtained from

$$K = \frac{4}{3\pi\left(\sigma_i + \sigma_j\right)}\left[\frac{R_i R_j}{R_i - R_j}\right]^{1/2},$$
$$\sigma_i = \frac{1 - \nu_i^2}{\pi E_i}, \tag{12}$$
$$\sigma_j = \frac{1 - \nu_j^2}{\pi E_j},$$

where ν and E are the Poisson ratio and Young modulus, respectively. R_i and R_j are radii of the joint elements.

The tangential contact of the clearance joint is represented using the friction force model. Here, a modified Coulomb friction model with dynamic friction coefficient is used for the tangential contact of the clearance joint, which can avoid numerical difficulties [5, 9, 14]. The expression of the modified Coulomb friction model is shown as

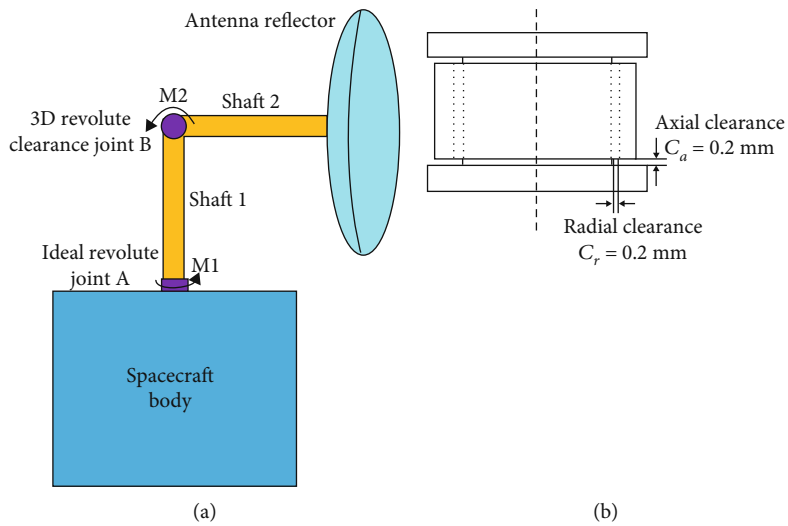

Figure 6: Schematic of satellite antenna system with 3D revolute clearance joint: (a) structure of the satellite antenna system; (b) 3D revolute clearance joint B with radial and axial clearances.

Table 1: Structural parameters of satellite antenna system.

	Mass (kg)	$\mathbf{I}_{xx}$ (kg·m^2)	$\mathbf{I}_{yy}$ (kg·m^2)	$\mathbf{I}_{zz}$ (kg·m^2)
Spacecraft body	2400	400	328	328
Shaft 1	4.712	0.1011	0.1011	0.00589
Shaft 2	4.712	0.1011	0.1011	0.00589
Antenna reflector	8.005	0.68297	1.05956	0.68297

$$F_t = -\mu(v_t) F_n \frac{v_t}{|v_t|}, \tag{13}$$

where the dynamic friction coefficient $\mu(v_t)$ is a function of tangential velocity and it is given as

$$\mu(v_t) = \begin{cases} -\mu_d \operatorname{sign}(v_t), & \text{for } |v_t| > v_d, \\ -\left\{\mu_d + (\mu_s - \mu_d)\left(\dfrac{|v_t| - v_s}{v_d - v_s}\right)^2 \left[3 - 2\left(\dfrac{|v_t| - v_s}{v_d - v_s}\right)\right]\right\} \operatorname{sign}(v_t), & \text{for } v_s \le |v_t| \le v_d, \\ \mu_s - 2\mu_s\left(\dfrac{v_t + v_s}{2v_s}\right)^2 \left(3 - \dfrac{v_t + v_s}{v_s}\right), & \text{for } |v_t| < v_s, \end{cases} \tag{14}$$

where v_t is the relative sliding velocity. μ_d and μ_s are dynamic and static friction coefficients, respectively. v_s and v_d are the given bounds for the tangential critical velocity.

Table 2: Parameters used in the dynamic simulation.

Parameters	Value
Driving moment of vertical axis (Nm)	$10\sin(2\pi t)$
Driving moment of horizontal axis (Nm)	$4\sin(2\pi t)$
Length of shaft 1 (m)	0.5
Length of shaft 2 (m)	0.5
Bearing length (m)	0.05
Bearing radius (m)	0.01
Bearing thickness (m)	0.002
Journal length (m)	0.054
Journal radius (m)	0.0098
Radius of journal flange (m)	0.014
Thickness of journal flange (m)	0.002
Radial clearance size (mm)	0.2
Axial clearance size (mm)	0.2
Static friction coefficient	0.15
Dynamic friction coefficient	0.1
Critical velocity of static friction (m/s)	0.1
Critical velocity of the maximum dynamic friction (m/s)	1.0
Restitution coefficient	0.9
Step size (s)	0.0001

4. Case Study and Results

4.1. Properties of the Satellite Antenna System. In this section, a space antenna system with spatial motion is used as the numerical example to investigate the effects of 3D revolute clearance joints on the dynamic responses of the satellite antenna system. Most of the previous studies focused on the dynamic responses of mechanisms with planar radial clearances and ignored the axial clearance. For a highly precise space mechanism with spatial motion, the effects of axial clearance in a revolute joint cannot be ignored. Therefore, first, we considered the case of the 3D revolute joint with radial clearance only. Second, we added the axial clearance to the 3D revolute joint with radial clearance. Then, we compared the simulation results for the case without axial clearance and the case with axial clearance to investigate the effects of axial clearance. Further, the effects of axial clearance size on dynamic characteristics of the space mechanism were discussed.

The main structure of the satellite antenna system consists of the spacecraft body, two shafts, two revolute joints, and a flexible antenna reflector, as shown in Figure 6. The

Table 3: Different case studies of 3D revolute clearance joint.

Cases	Description	Clearance size (mm)
Case 1	Ideal revolute joint without clearance	$C_r = C_a = c = 0$
Case 2	3D revolute joint with radial clearance	$C_r = 0.2$, $C_a = 0$
Case 3	3D revolute joint with both radial and axial clearances	$C_r = C_a = c = 0.2$

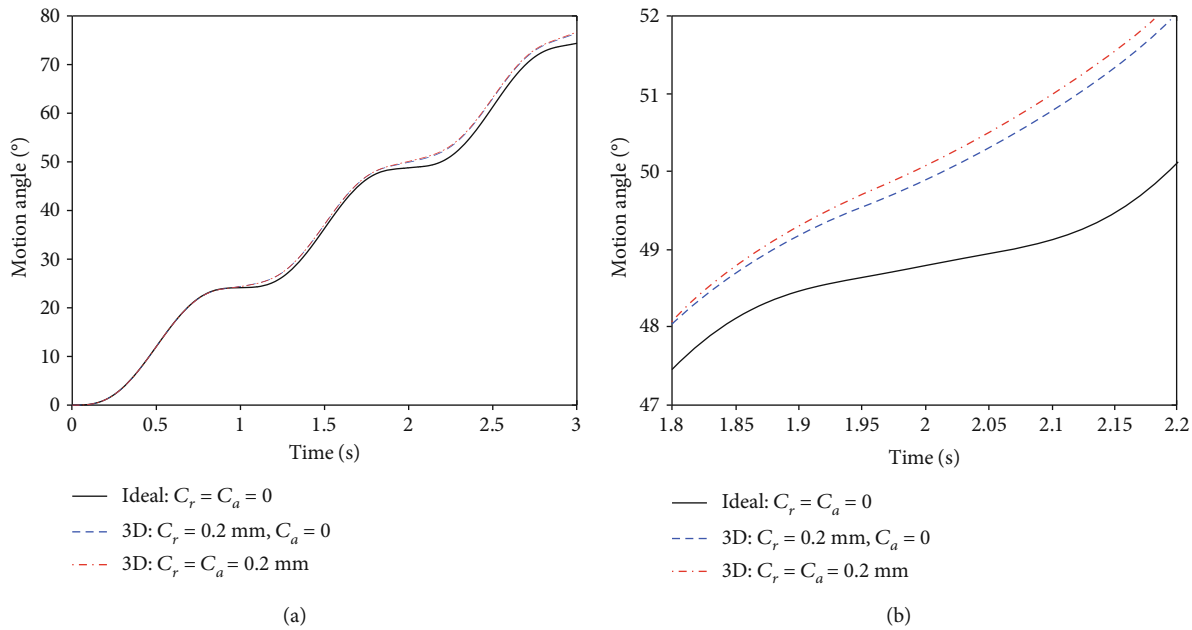

Figure 7: Motion angular displacement of the antenna: (a) motion angle; (b) partial zoom.

satellite antenna system is a spatial mechanism with two degrees of freedom. The two shafts are crossed and vertical in the initial status. The antenna reflector is modeled as a flexible body, which is fixed together with the end shaft 2. Other bodies are considered as rigid bodies. In the dynamic simulation, the 3D revolute clearance joint exists between the two shafts, and initially, the axes of the journal and the bearing of the 3D revolute clearance joint are coincident. The dynamics simulations for the satellite antenna system with the 3D revolute clearance joint and the ideal system without clearance are presented. The structural parameters of satellite antenna system are shown in Table 1, and the parameters used in the dynamics simulation are shown in Table 2.

4.2. Effects of the 3D Revolute Clearance Joints on the Satellite Antenna System

4.2.1. Effects of 3D Revolute Clearance Joint. In this section, three case studies, as listed in Table 3, are presented with different initial configurations to investigate the effects of the 3D revolute clearance joint on the dynamic performances of the satellite antenna.

In the first case study, the revolute joint is considered as an ideal joint, that is, there are no clearances in the revolute joint. In the second case study, there is only radial clearance considered in the 3D revolute clearance joint and there is no axial clearance. In the third case, both the radial and axial clearances exist in the 3D revolute clearance joint. The effects of the axial clearance are investigated.

The simulation results are presented as Figures 7–9, which show the angle displacement, angular velocity, and angular acceleration of the satellite antenna system. Figure 10 presents the contact forces in the revolute clearance joint.

Figure 7 shows that the clearance will lead to deviation of the motion angle compared with that of the ideal case. When the revolute joint is considered as the 3D revolute clearance joint considering both the radial and axial clearances, the deviations of the motion displacement of the antenna are increased. Thus, it decreases the motion accuracy of the satellite antenna when the axial clearance is also considered in the 3D revolute clearance joint. Figure 8 shows that the effects of clearances on angular velocity are much more obvious. The angular velocity is shaky and deviates from the ideal case without clearances. When both the radial and axis clearances are considered in the 3D revolute joint, the deviations of the antenna motion are bigger than that of only the radial clearance considered in the 3D revolute joint. Figure 9 shows that, when both the radial and axial clearances are considered in the 3D revolute clearance joint, the shake of the satellite antenna is extraordinarily obvious. The shaky peaks of the

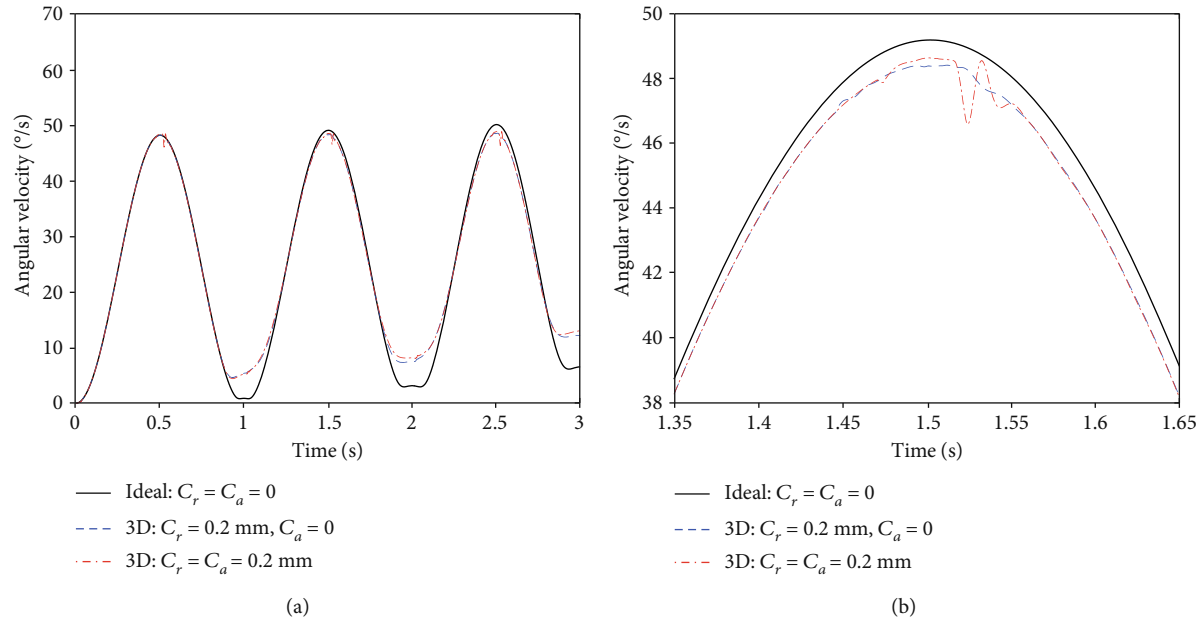

Figure 8: Angular velocity of the antenna: (a) angular velocity; (b) partial zoom.

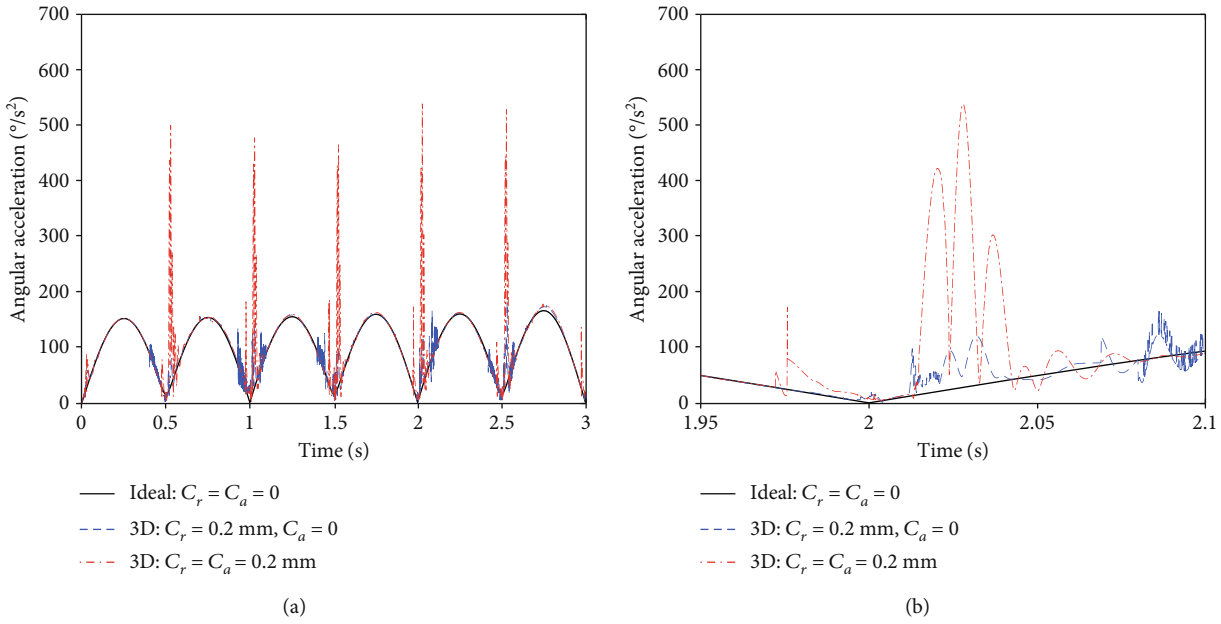

Figure 9: Angular acceleration of the antenna: (a)angular acceleration; (b) partial zoom.

angular acceleration of the satellite antenna increase sharply compared with those of only the radial clearance considered in the revolute joint.

The reasons are that clearances in the joint lead to contact and impact forces in the clearance joint for the spatial motion of the satellite antenna, as shown in Figure 10. It clearly shows that clearances lead to impulse type contact forces and the contact forces are high-frequency shaky with high peaks. Comparing with Figures 10(a)–10(c) shows that the existence of the axial clearance in the 3D revolute clearance joint leads to more severe effects, especially in the axial direction of the contact forces. The contact forces in the axial direction are increased sharply with much higher shaky peaks than that of only considering radial clearance. It indicates that the existence of clearances will lead to undesirable vibrations of the satellite antenna and influence the movement stability of the satellite antenna, especially when the axial clearance is also considered in the revolute joint. The 3D revolute clearance joint will lead to more severe effects on the dynamic performances of the satellite antenna when both the radial and axial clearances are considered. Therefore, the effects of axial clearance on the satellite antenna cannot be ignored in the dynamics analysis of the satellite antenna system.

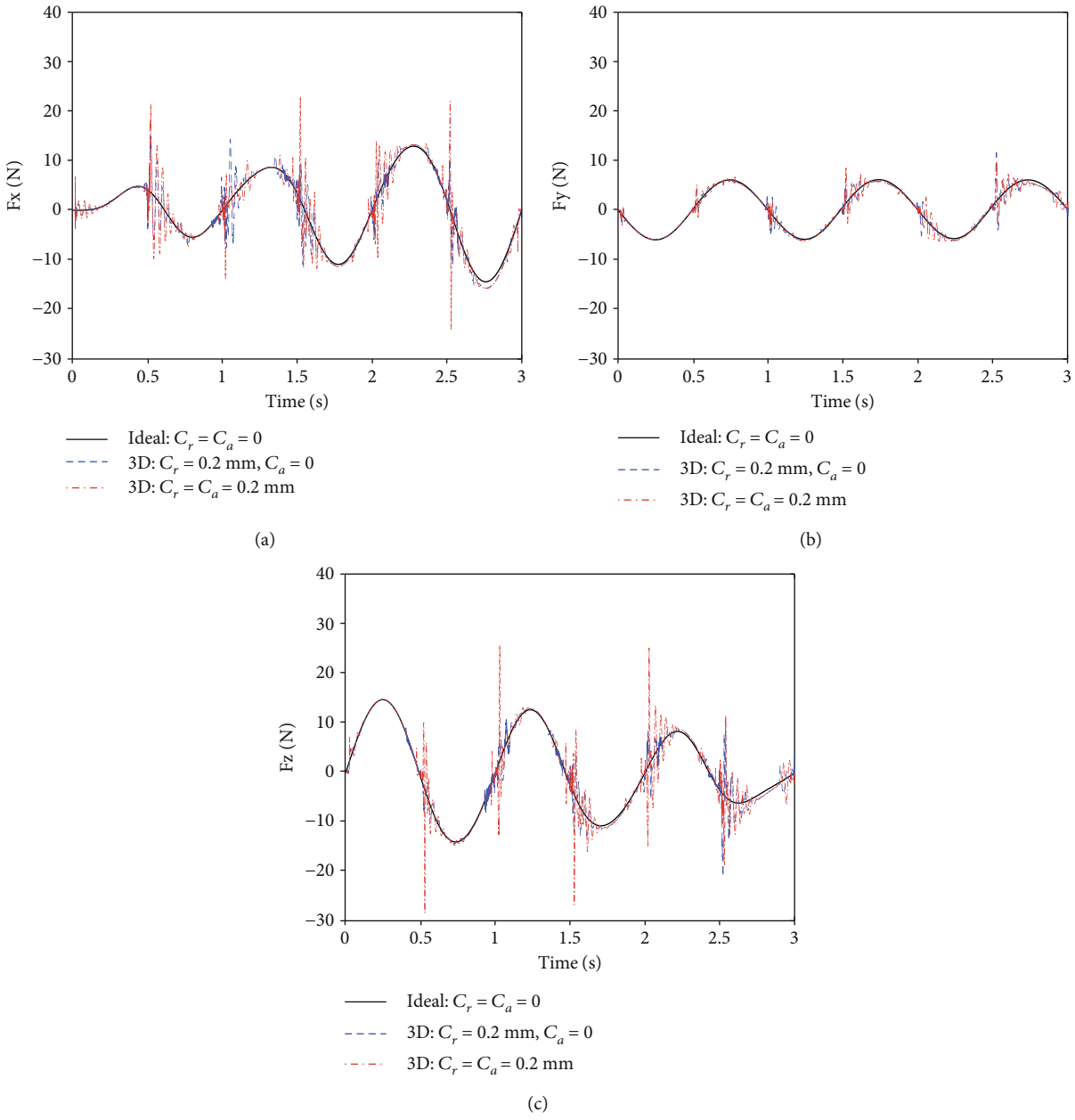

Figure 10: Contact forces in 3D revolute clearance joint.

Table 4: Different axial clearance sizes of 3D revolute clearance joint.

Cases	Description	Clearance size (mm)
Case 1	Ideal revolute joint without clearance	$C_r = C_a = c = 0$
Case 2	3D revolute clearance joint	$C_r = 0.2$, $C_a = 0$
Case 3	3D revolute clearance joint	$C_r = 0.2$, $C_a = 0.2$
Case 4	3D revolute clearance joint	$C_r = 0.2$, $C_a = 0.3$
Case 5	3D revolute clearance joint	$C_r = 0.2$, $C_a = 0.4$

Meanwhile, the simulation results are compared to other studies from previous literatures on planar and spatial revolute clearance joints [9, 10, 23, 61–63]. The previous researches showed that the planar revolute joint with radial clearance had important effects on the dynamic responses, especially the acceleration of multibody mechanical systems. Also, the previous studies indicated that the 3D revolute clearance joint will lead to more significant effects on dynamic responses of mechanism systems. Therefore, the simulation results are validated by other data published on the field of dynamics of mechanism systems with clearance joints.

4.2.2. Effects of Axial Clearance Size. In this section, the effects of the axial clearance size of the 3D revolute clearance

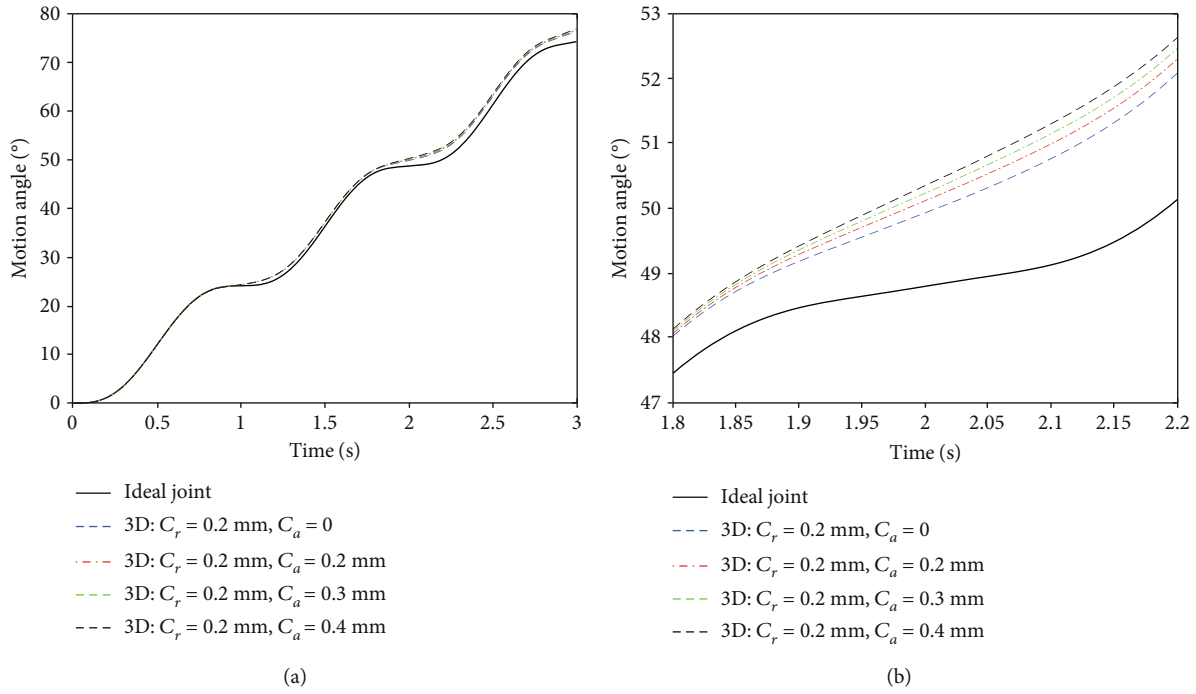

Figure 11: Motion angular displacement of the antenna: (a) motion angle; (b) partial zoom.

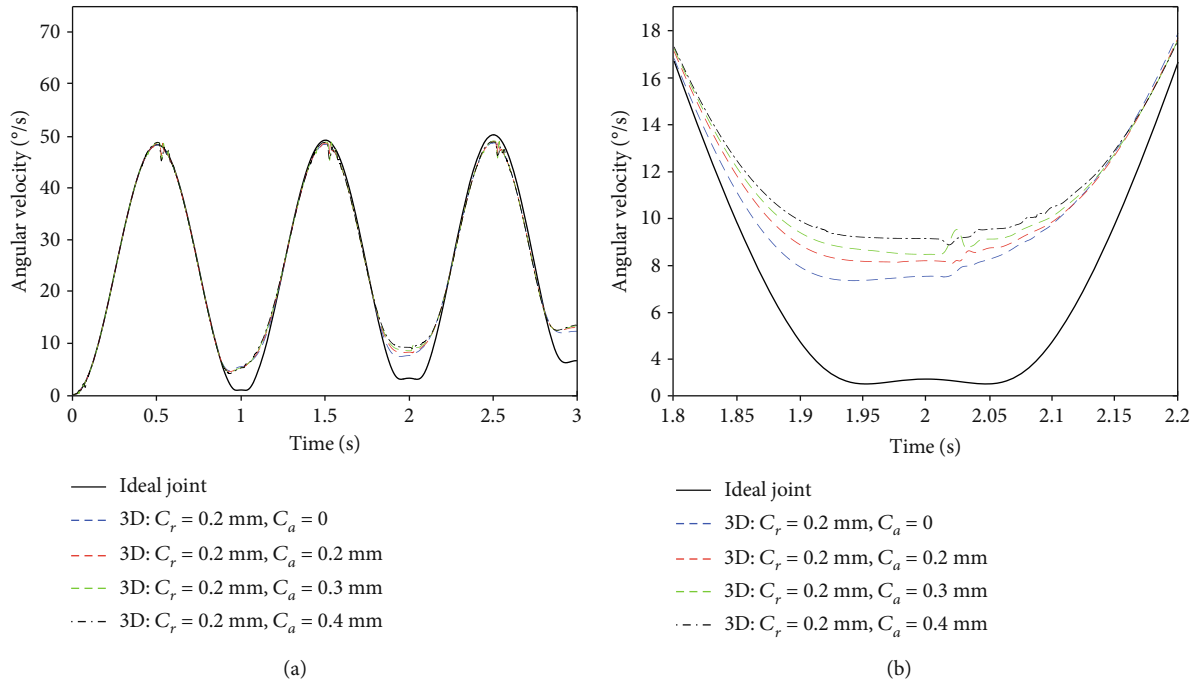

Figure 12: Angular velocity of the antenna: (a) angular velocity; (b) partial zoom.

joint are investigated. Five case studies are presented, as shown in Table 4. The simulation results are presented in Figures 11–13. It also can be found that the bigger size of the axial clearance will induce more severe shaky responses and much higher shaky peaks. Therefore, a bigger size of the axial clearance will lead to worse performance of the satellite antenna system.

The fact that the existence of both the radial and axial clearances in 3D revolute clearance joints has an important effect on the dynamic performances of the satellite antenna supports the idea that the axial clearance in the revolute joint cannot be ignored. The axial clearance in a 3D revolute clearance joint must be considered in the dynamics analysis and design of the real satellite antenna systems.

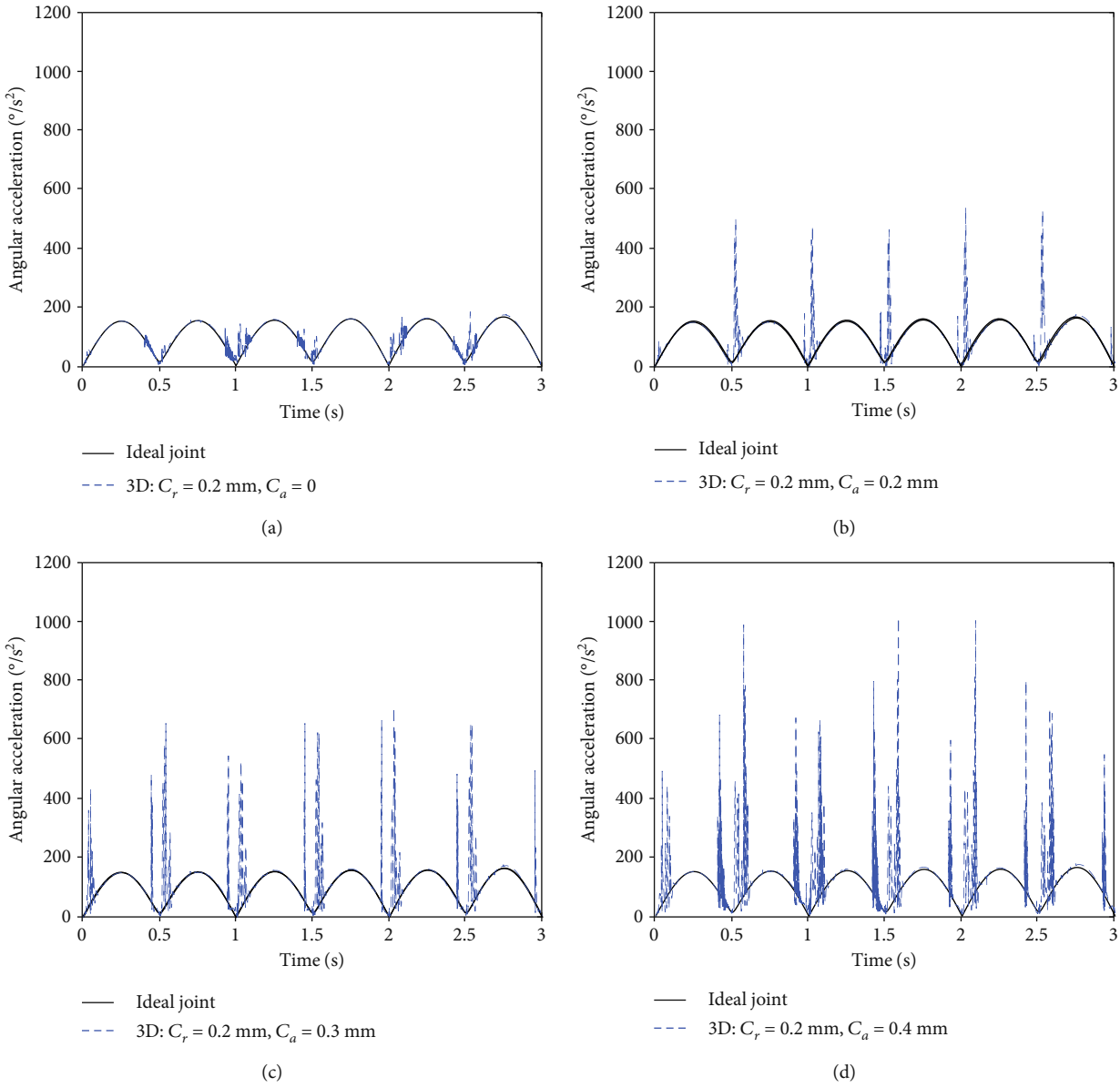

Figure 13: Angular acceleration of antenna: (a) $C_r = 0.2$ mm, $C_a = 0$; (b) $C_r = 0.2$ mm, $C_a = 0.2$ mm; (c) $C_r = 0.2$ mm, $C_a = 0.3$ mm; (d) $C_r = 0.2$ mm, $C_a = 0.4$ mm.

5. Conclusions

Generally, axial clearances always exist in revolute joints due to the manufacturing and assembling errors, which have been less considered. However, axial clearances will result in relative motion along the axial direction between the journal and bearing of a 3D revolute clearance joint. Correspondingly, it will influence the dynamic characteristics of mechanisms. In this paper, a methodology for modeling the 3D revolute joint with clearance and its application in satellite antenna system are presented.

The mechanical bodies connected by the 3D revolute clearance joint are modelled as contact rigid bodies, and it is modelled as contact force constraints. Consequently, contact-impact forces control the dynamics of the clearance joint. For a 3D spatial revolute clearance joint, there will be 13 potential contact scenarios, which can reveal the different contact phenomena. A satellite antenna system with spatial motion is presented as the demonstrative application example. Then, the dynamic characteristics of the space antenna system considering both the radial and axial clearances in the 3D revolute clearance joints are investigated. Different case studies are presented and discussed.

The numerical simulation results indicate that (1) the dynamic responses of the antenna system are obviously shaky with much higher peaks when considering both the radial and axial clearance. Therefore, the 3D revolute clearance joint leads to much more severe effects on the dynamic performances of the satellite antenna system. (2) The contact forces exist in both the radial and axial directions. The existence of the axial clearance in the 3D revolute clearance joint leads to more severe effects on the 3D revolute clearance

joint, which will induce undesirable vibrations and affect the movement stability and accuracy of the satellite antenna. (3) The bigger size of the axial clearance will induce much more severe shaky responses and much higher shaky peaks.

Clearances in revolute joints play a crucial role in predicting accurately the dynamic responses of the satellite antenna system. The studies of this paper indicate that the effects of the axial clearance on the satellite antenna system cannot be ignored. The methodology for modeling the 3D revolute joint with clearances is the basis of performance analysis and system design of space mechanisms, which develops the revolute joint to real engineering application.

Data Availability

The data used to support the findings of this study are included within the article.

Conflicts of Interest

The authors declare that there is no conflict of interest regarding the publication of this paper.

Acknowledgments

This work is supported by the National Natural Science Foundation of China (Grant Nos. 51775128 and 51305093).

References

[1] X. S. Sun, D. Yang, Y. H. Geng, and X. Yang, "The antenna pointing control strategy study of tracking and data relay satellite," *Acta Aeronautica Et Astronautica Sinica*, vol. 25, no. 4, pp. 376–380, 2004.

[2] J. Sun, X. R. Ma, and D. Y. Yu, "Pointing accuracy analyses of a satellite two-axes antenna pointing mechanism," *Journal of Astronautics*, vol. 28, no. 3, pp. 545–550, 2007.

[3] B. You, H. Zhang, W. Li, Z. Zhao, and J. Chen, "Dynamic analysis of satellite antenna system with joint clearance and reflector flexibility," *Journal of Aerospace Engineering*, vol. 27, no. 2, pp. 297–307, 2014.

[4] Z. F. Bai, Y. Q. Liu, and Y. Sun, "Investigation on dynamic responses of dual-axis positioning mechanism for satellite antenna considering joint clearance," *Journal of Mechanical Science and Technology*, vol. 29, no. 2, pp. 453–460, 2015.

[5] Z. F. Bai, J. J. Zhao, J. Chen, and Y. Zhao, "Design optimization of dual-axis driving mechanism for satellite antenna with two planar revolute clearance joints," *Acta Astronautica*, vol. 144, pp. 80–89, 2018.

[6] P. Flores, "Modeling and simulation of wear in revolute clearance joints in multibody systems," *Mechanism and Machine Theory*, vol. 44, no. 6, pp. 1211–1222, 2009.

[7] S. Mukras, N. H. Kim, N. A. Mauntler, T. L. Schmitz, and W. G. Sawyer, "Analysis of planar multibody systems with revolute joint wear," *Wear*, vol. 268, no. 5-6, pp. 643–652, 2010.

[8] L. X. Zhang, Z. F. Bai, Y. Zhao, and X. B. Cao, "Dynamic response of solar panel deployment on spacecraft system considering joint clearance," *Acta Astronautica*, vol. 81, no. 1, pp. 174–185, 2012.

[9] Z. F. Bai and Y. Zhao, "Dynamic behaviour analysis of planar mechanical systems with clearance in revolute joints using a new hybrid contact force model," *International Journal of Mechanical Sciences*, vol. 54, no. 1, pp. 190–205, 2012.

[10] B. Brogliato, "Feedback control of multibody systems with joint clearance and dynamic backlash: a tutorial," *Multibody System Dynamics*, vol. 42, no. 3, pp. 283–315, 2018.

[11] Z. F. Bai, Y. Zhao, and J. Chen, "Dynamics analysis of planar mechanical system considering revolute clearance joint wear," *Tribology International*, vol. 64, pp. 85–95, 2013.

[12] B. Zhao, X. D. Dai, Z. N. Zhang, S.-H. Wu, and Y.-B. Xie, "Numerical study of parametric effects on joint wear in the flexible multibody systems with different flexibilities and clearance sizes," *Proceedings of the Institution of Mechanical Engineers, Part J: Journal of Engineering Tribology*, vol. 228, no. 8, pp. 819–835, 2014.

[13] K. L. Ting, J. D. Zhu, and D. Watkins, "The effects of joint clearance on position and orientation deviation of linkages and manipulators," *Mechanism and Machine Theory*, vol. 35, no. 3, pp. 391–401, 2000.

[14] Z. F. Bai and Y. Zhao, "Dynamics modeling and quantitative analysis of multibody systems including revolute clearance joint," *Precision Engineering*, vol. 36, no. 4, pp. 554–567, 2012.

[15] Y. Li, Z. Wang, C. Wang, and W. Huang, "Effects of torque spring, CCL and latch mechanism on dynamic response of planar solar arrays with multiple clearance joints," *Acta Astronautica*, vol. 132, pp. 243–255, 2017.

[16] C. Xiulong, J. Yonghao, D. Yu, and W. Qing, "Dynamics behavior analysis of parallel mechanism with joint clearance and flexible links," *Shock and Vibration*, vol. 2018, Article ID 9430267, 17 pages, 2018.

[17] S. Rahmanian and M. R. Ghazavi, "Bifurcation in planar slider-crank mechanism with revolute clearance joint," *Mechanism and Machine Theory*, vol. 91, pp. 86–101, 2015.

[18] J. Li, H. Huang, S. Yan, and Y. Yang, "Kinematic accuracy and dynamic performance of a simple planar space deployable mechanism with joint clearance considering parameter uncertainty," *Acta Astronautica*, vol. 136, pp. 34–45, 2017.

[19] X. Zhang, R. Zhang, and Q. Wang, "Comparison and analysis of two Coulomb friction models on the dynamic behavior of slider-crank mechanism with a revolute clearance joint," *Applied Mathematics and Mechanics*, vol. 39, no. 9, pp. 1239–1258, 2018.

[20] D. Sun, Y. Shi, and B. Zhang, "Robust optimization of constrained mechanical system with joint clearance and random parameters using multi-objective particle swarm optimization," *Structural and Multidisciplinary Optimization*, vol. 58, no. 5, pp. 2073–2084, 2018.

[21] Y. Li, C. Wang, and W. Huang, "Rigid-flexible-thermal analysis of planar composite solar array with clearance joint considering torsional spring, latch mechanism and attitude controller," *Nonlinear Dynamics*, vol. 96, no. 3, pp. 2031–2053, 2019.

[22] M. Qian, Z. Qin, S. Yan, and L. Zhang, "A comprehensive method for the contact detection of a translational clearance joint and dynamic response after its application in a crank-slider mechanism," *Mechanism and Machine Theory*, vol. 145, article 103717, 2020.

[23] P. Flores, "A parametric study on the dynamic response of planar multibody systems with multiple clearance joints," *Nonlinear Dynamics*, vol. 61, no. 4, pp. 633–653, 2010.

[24] Y. Zhao and Z. F. Bai, "Dynamics analysis of space robot manipulator with joint clearance," *Acta Astronautica*, vol. 68, no. 7-8, pp. 1147–1155, 2011.

[25] S. Erkaya and I. Uzmay, "Determining link parameters using genetic algorithm in mechanisms with joint clearance," *Mechanism and Machine Theory*, vol. 44, no. 1, pp. 222–234, 2009.

[26] S. Erkaya and I. Uzmay, "Experimental investigation of joint clearance effects on the dynamics of a slider-crank mechanism," *Multibody System Dynamics*, vol. 24, no. 1, pp. 81–102, 2010.

[27] O. Muvengei, J. Kihiu, and B. Ikua, "Dynamic analysis of planar rigid-body mechanical systems with two-clearance revolute joints," *Nonlinear Dynamics*, vol. 73, no. 1-2, pp. 259–273, 2013.

[28] Z. F. Bai and Y. Sun, "A study on dynamics of planar multibody mechanical systems with multiple revolute clearance joints," *European Journal of Mechanics - A/Solids*, vol. 60, pp. 95–111, 2016.

[29] G. Wang, Z. Qi, and J. Wang, "A differential approach for modeling revolute clearance joints in planar rigid multibody systems," *Multibody System Dynamics*, vol. 39, no. 4, pp. 311–335, 2017.

[30] X. Zhang and X. Zhang, "Minimizing the influence of revolute joint clearance using the planar redundantly actuated mechanism," *Robotics and Computer-Integrated Manufacturing*, vol. 46, pp. 104–113, 2017.

[31] E. Salahshoor, S. Ebrahimi, and Y. Zhang, "Frequency analysis of a typical planar flexible multibody system with joint clearances," *Mechanism and Machine Theory*, vol. 126, pp. 429–456, 2018.

[32] X. Wang, G. Liu, S. Ma, and R. Tong, "Study on dynamic responses of planar multibody systems with dry revolute clearance joint: numerical and experimental approaches," *Journal of Sound and Vibration*, vol. 438, pp. 116–138, 2019.

[33] H. Tan, Y. Hu, and L. Li, "Effect of friction on the dynamic analysis of slider-crank mechanism with clearance joint," *International Journal of Mechanical Sciences*, vol. 115, pp. 20–40, 2019.

[34] X. Chen, S. Jiang, S. Wang, and Y. Deng, "Dynamics analysis of planar multi-DOF mechanism with multiple revolute clearances and chaos identification of revolute clearance joints," *Multibody System Dynamics*, vol. 47, no. 4, pp. 317–345, 2019.

[35] Y. Li, C. Wang, and W. Huang, "Dynamics analysis of planar rigid-flexible coupling deployable solar array system with multiple revolute clearance joints," *Mechanical Systems and Signal Processing*, vol. 117, pp. 188–209, 2019.

[36] G. Wang and L. Wang, "Dynamics investigation of spatial parallel mechanism considering rod flexibility and spherical joint clearance," *Mechanism and Machine Theory*, vol. 137, pp. 83–107, 2019.

[37] T. Pi and Y. Zhang, "Simulation of planar mechanisms with revolute clearance joints using the multipatch based isogeometric analysis," *Computer Methods in Applied Mechanics and Engineering*, vol. 343, pp. 453–489, 2019.

[38] A. Amiri, M. Dardel, and H. M. Daniali, "Effects of passive vibration absorbers on the mechanisms having clearance joints," *Multibody System Dynamics*, vol. 47, no. 4, pp. 363–395, 2019.

[39] Z. Zhan, X. Zhang, H. Zhang, and G. Chen, "Unified motion reliability analysis and comparison study of planar parallel manipulators with interval joint clearance variables," *Mechanism and Machine Theory*, vol. 138, pp. 58–75, 2019.

[40] J. Guo, R. B. Randall, P. Borghesani, W. A. Smith, M. D. Haneef, and Z. Peng, "A study on the effects of piston secondary motion in conjunction with clearance joints," *Mechanism and Machine Theory*, vol. 149, article 103824, 2020.

[41] Y. Chen, J. Feng, X. Peng, Y. Sun, Q. He, and C. Yu, "An approach for dynamic analysis of planar multibody systems with revolute clearance joints," *Engineering with Computers*, vol. 36, 2020.

[42] S. Erkaya, "Effects of joint clearance on the motion accuracy of robotic manipulators," *Strojniški vestnik - Journal of Mechanical Engineering*, vol. 64, pp. 82–94, 2018.

[43] S. Yan and P. Guo, "Kinematic accuracy analysis of flexible mechanisms with uncertain link lengths and joint clearances," *Proceedings of the Institution of Mechanical Engineers, Part C: Journal of Mechanical Engineering Science*, vol. 225, no. 8, pp. 1973–1983, 2011.

[44] A. Chaker, A. Mlika, M. A. Laribi, L. Romdhane, and S. Zeghloul, "Clearance and manufacturing errors' effects on the accuracy of the 3-RCC spherical parallel manipulator," *European Journal of Mechanics - A/Solids*, vol. 37, pp. 86–95, 2013.

[45] W. Xiang and S. Yan, "Dynamic analysis of space robot manipulator considering clearance joint and parameter uncertainty: modeling, analysis and quantification," *Acta Astronautica*, vol. 169, pp. 158–169, 2020.

[46] W. Xiang, S. Yan, J. Wu, and W. Niu, "Dynamic response and sensitivity analysis for mechanical systems with clearance joints and parameter uncertainties using Chebyshev polynomials method," *Mechanical Systems and Signal Processing*, vol. 138, article 106596, 2020.

[47] Q. Zhao, J. Guo, and J. Hong, "Closed-form error space calculation for parallel/hybrid manipulators considering joint clearance, input uncertainty, and manufacturing imperfection," *Mechanism and Machine Theory*, vol. 142, article 103608, 2019.

[48] Z. F. Bai, Y. Zhao, and X. G. Wang, "Wear analysis of revolute joints with clearance in multibody systems," *Science China Physics, Mechanics and Astronomy*, vol. 56, no. 8, pp. 1581–1590, 2013.

[49] X. Lai, H. He, Q. Lai et al., "Computational prediction and experimental validation of revolute joint clearance wear in the low-velocity planar mechanism," *Mechanical Systems and Signal Processing*, vol. 85, pp. 963–976, 2017.

[50] S. Erkaya, "Trajectory optimization of a walking mechanism having revolute joints with clearance using ANFIS approach," *Nonlinear Dynamics*, vol. 71, no. 1-2, pp. 75–91, 2013.

[51] G. B. Daniel and K. L. Cavalca, "Analysis of the dynamics of a slider-crank mechanism with hydrodynamic lubrication in the connecting rod-slider joint clearance," *Mechanism and Machine Theory*, vol. 46, no. 10, pp. 1434–1452, 2011.

[52] B. Zhao, Z. N. Zhang, C. C. Fang, X. D. Dai, and Y. B. Xie, "Modeling and analysis of planar multibody system with mixed lubricated revolute joint," *Tribology International*, vol. 98, pp. 229–241, 2016.

[53] Z. F. Bai, X. Shi, and P. P. Wang, "Effects of body flexibility on dynamics of mechanism with clearance joint," *Lecture Notes in Electrical Engineering*, vol. 408, pp. 1239–1247, 2017.

[54] I. Khemili and L. Romdhane, "Dynamic analysis of a flexible slider–crank mechanism with clearance," *European Journal of Mechanics - A/Solids*, vol. 27, no. 5, pp. 882–898, 2008.

[55] S. B. Farahan, M. R. Ghazavi, and S. Rahmanian, "Bifurcation in a planar four-bar mechanism with revolute clearance joint," *Nonlinear Dynamics*, vol. 87, pp. 955–973, 2017.

[56] O. Muvengei, J. Kihiu, and B. Ikua, "Dynamic analysis of planar multi-body systems with LuGre friction at differently located revolute clearance joints," *Multibody System Dynamics*, vol. 28, pp. 369–393, 2012.

[57] X. Zheng, J. Li, Q. Wang, and Q. Liao, "A methodology for modeling and simulating frictional translational clearance joint in multibody systems including a flexible slider part," *Mechanism and Machine Theory*, vol. 142, article 103603, 2019.

[58] Q. Zhao, J. Guo, J. Hong, and Z. Liu, "Analysis of angular errors of the planar multi-closed-loop deployable mechanism with link deviations and revolute joint clearances," *Aerospace Science and Technology*, vol. 87, pp. 25–36, 2019.

[59] C. Jin, L. Fan, and Y. Qiu, "The vibration control of a flexible linkage mechanism with impact," *Communications in Nonlinear Science and Numerical Simulation*, vol. 9, no. 4, pp. 459–469, 2004.

[60] P. Flores, C. S. Koshy, H. M. Lankarani, J. Ambrósio, and J. C. P. Claro, "Numerical and experimental investigation on multibody systems with revolute clearance joints," *Nonlinear Dynamics*, vol. 65, no. 4, pp. 383–398, 2011.

[61] P. Flores, J. Ambrósio, J. P. Claro, and H. M. Lankarani, "Spatial revolute joints with clearances for dynamic analysis of multi-body systems," *Proceedings of the Institution of Mechanical Engineers, Part K: Journal of Multi-body Dynamics*, vol. 220, pp. 257–271, 2016.

[62] C. Brutti, G. Coglitore, and P. P. Valentini, "Modeling 3D revolute joint with clearance and contact stiffness," *Nonlinear Dynamics*, vol. 66, no. 4, pp. 531–548, 2011.

[63] S. Yan, W. Xiang, and L. Zhang, "A comprehensive model for 3D revolute joints with clearances in mechanical systems," *Nonlinear Dynamics*, vol. 80, no. 1-2, pp. 309–328, 2015.

[64] F. Marques, F. Isaac, N. Dourado, and P. Flores, "An enhanced formulation to model spatial revolute joints with radial and axial clearances," *Mechanism and Machine Theory*, vol. 116, pp. 123–144, 2017.

[65] F. Isaac, F. Marques, N. Dourado, and P. Flores, "A finite element model of a 3D dry revolute joint incorporated in a multibody dynamic analysis," *Multibody System Dynamics*, vol. 45, no. 3, pp. 293–313, 2019.

[66] D. S. Lopes, M. T. Silva, J. A. Ambrósio, and P. Flores, "A mathematical framework for rigid contact detection between quadric and superquadric surfaces," *Multibody System Dynamics*, vol. 24, no. 3, pp. 255–280, 2010.

[67] Q. Tian, P. Flores, and H. M. Lankarani, "A comprehensive survey of the analytical, numerical and experimental methodologies for dynamics of multibody mechanical systems with clearance or imperfect joints," *Mechanism and Machine Theory*, vol. 122, pp. 1–57, 2018.

[68] K. H. Hunt and F. R. E. Crossley, "Coefficient of restitution interpreted as damping in vibroimpact," *Journal of Applied Mechanics*, vol. 42, no. 2, pp. 440–445, 1975.

[69] Z. F. Bai and Y. Zhao, "A hybrid contact force model of revolute joint with clearance for planar mechanical systems," *International Journal of Non-Linear Mechanic*, vol. 48, pp. 15–36, 2013.

[70] P. Flores, J. Ambrósio, J. C. P. Claro, and H. M. Lankarani, *Kinematics and Dynamics of Multibody Systems with Imperfect Joints: Models and Case Studies*, Springer, 2007.

[71] P. Flores, J. Ambrósio, J. C. P. Claro, and H. M. Lankarani, "Influence of the contact-impact force model on the dynamic response of multibody systems," *Proceedings of the Institution of Mechanical Engineers, Part K: Journal of Multi-body Dynamics*, vol. 220, no. 1, pp. 21–34, 2006.

[72] H. M. Lankarani and P. E. Nikravesh, "A contact force model with hysteresis damping for impact analysis of multibody systems," *Journal of Mechanical Design*, vol. 112, pp. 69–376, 1990.

[73] C. S. Koshy, P. Flores, and H. M. Lankarani, "Study of the effect of contact force model on the dynamic response of mechanical systems with dry clearance joints: computational and experimental approaches," *Nonlinear Dynamics*, vol. 73, no. 1-2, pp. 325–338, 2013.